621.793.002.3-419:533.273

K. S. Kim, H. K. Kim, J. H. La, K. B. Kim, S. Y. Lee*
Center for Surface Technology and Applications,
Department of Materials Engineering, Korea Aerospace University,
GoYang-si, Gyeonggi-do, South Korea
**sylee@kau.ac.kr*

Influence of N_2 partial pressure on the microstructure, hardness, and thermal stability of CrZrSiN nanocomposite coatings

The effects of N_2 partial pressure in the unbalanced magnetron sputtering process on the microstructure, hardness, and thermal stability of the CrZrSiN nanocomposite coating were investigated. A typical nanocomposite structure, composed of a crystalline phase and an amorphous phase was obtained and the distribution of these phases changed with increasing N_2 partial pressure. The N_{1s} spectra revealed the presence of two-peak characteristic of nitrogen in the CrZrN and SiN_x phases, and the ratio of the peak's SiN_x to CrZrN intensity increased with increasing N_2 partial pressure, indicating an increase in the amorphous phase in the nanocomposite microstructure. As N_2 partial pressure increased, the CrZrSiN coating hardness decreased from 38 to 30 GPa due to the increasing amount of the SiN_x amorphous phase. After the thermal stability test, the hardness values of the CrZrSiN coatings were maintained at approximately 30 GPa up to 800 °C, but the hardness decreased rapidly to 18 GPa after annealing at 900 °C. This drastic change of hardness over 900 °C was due to the formation of a Cr_2O_3 phase in the CrZrSiN coating.

Keywords: *coating, nanocomposite, microstructure, amorphous phase.*

INTRODUCTION

Over the last decade, hard coatings have been applied extensively to various types of cutting tools to improve their lifetime and performance, enhance productivity, and enable specific engineering applications. However, the performance of coatings could degrade seriously in high-temperature environment. Recently, significant developments have been made in the field of hard coatings in order to overcome the limitations of conventional nitride coatings. In particular, numerous scientific and technologic efforts have been devoted to research on nanocomposite coatings. Past studies on these Si-containing nitrides [1–5] reported that the incorporation of Si resulted in a refinement of the grain size of the crystalline MeN phase (Me = Metal) and the formation of a SiN_x phase. This consequently led to the formation of two phases in nanocomposite structures: a nanocrystalline and an amorphous phase. At the nanocrystalline phase, which has very small grain sizes, any dislocation movement that arises is trapped at the grain boundaries. Also, the amorphous layer plays an important role as a diffusion barrier that inhibits the diffusion of the oxygen ions [6]. For these reasons, nanocomposite coatings are able to simultaneously obtain greater hardness and enhanced thermal stability. To optimize the excellent performance potential of

nanocomposite coatings, it is important to control the microstructure in the nanocomposite coating composed of the crystalline phase and the amorphous phase.

In previous works, Si content, high temperatures and substrate bias voltage were used to change the nanocomposite structure in the coating. Considerable research has shown that the nanocomposite structure is affected by the Si content in the coatings [7, 8]. Veprek [9] suggested that high temperature was necessary to achieve a Si-containing nanocomposite structure. Zhang et al. [10] concluded that the hardness and microstructure of Si-containing nanocomposite coatings changed with varying substrate bias voltages. However, little attention has been given to controlling a nanocomposite structure using N_2 partial pressure.

Most recently, TiAlSiN, AlCrSiN, and CrZrSiN nanocomposite coatings have been found to have even better practical performance capabilities compared to those of nanocrystalline coatings [11–13]. CrZrSiN coatings are especially promising; they have excellent mechanical properties and a low friction coefficient at high temperatures. Previous studies have looked at the influence of Si or Zr content on the microstructure, mechanical, and electrochemical properties of CrZrSiN coatings [14, 15]. In the present study, the effect of N_2 partial pressure on the microstructure and mechanical properties of CrZrSiN nanocomposite coatings is investigated.

EXPERIMENTAL

CrZrSiN coatings were deposited on (100) silicon wafer using a closed-field unbalanced magnetron sputtering system. A high purity Cr–Zr–Si segment target (99.9 %) was used for the deposition of the coatings. Prior to the deposition, the substrates were cleaned with acetone in an ultrasonic vessel for 30 minutes. The base pressure was pumped down to less than $2.0 \cdot 10^{-3}$ Pa and pre-sputtering was carried out for 10 minutes to clean the target surface at an Ar pressure of 0.39 Pa. During the deposition, a total working pressure of 0.61 Pa was obtained. Ar and N_2 were bled into the chamber with different N_2 partial pressures (from 0.16 to 0.31 Pa). In other deposition conditions, a DC substrate bias of –100 V was applied and the chamber temperature was maintained at 150 °C.

The crystalline phase of the CrZrSiN coating was analyzed using an X-ray diffractometer (Rigaku, SmartLAB) with monochromatic Cu$K\alpha$ (λ = 0.15456 nm) radiation operated at 30 kV. The analyzed range of the diffraction angle 2θ was between 20° and 80° using a step of 0.16°. X-ray photoelectron spectroscopy (Thermo Fisher Scientific, K-ALPHA) was also performed to observe the bonding status in the CrZrSiN coating. The hardness and elastic modulus of the coatings were measured using a Fischer scope (Helmut Fischer, HM2000) with a load of 25 mN and dwelling time of 30 seconds. In order to avoid the substrate effect, the indentation depth was kept to be less than approximately 0.18 μm, which was less than 10 % of the total coating thickness. A field emission scanning electron microscope (JEOL, JSM-7100F) and transmission electron microscope (JEOL, JEM-ARM 200F) were employed to study the microstructure of the CrZrSiN coatings. An annealing test was performed to evaluate the thermal stability of the coatings. The CrZrSiN coatings were annealed at temperatures from 500 to 1000 °C in air for 30 min. After the annealing test, the hardness was investigated. A Raman spectrometer (HORIBA, Lab Ram ARAMIS) was used and a He-Ne laser beam was used as the excitation source.

RESULTS AND DISCUSSION

Cross sectional images of the CrZrSiN coatings deposited on the Si wafer at various N_2 partial pressures are shown in Fig. 1. The CrZrSiN coatings show featureless structures in all conditions. The deposition rate decreases with increasing N_2 partial pressures. As the N_2 partial pressure increased by two times, the thickness of the coating decreased from 3.6 to 1.8 μm. This occurred because the reactive gas would react with the sputter targets to form a nitride compound layer at the surface. The nitride layer on the target surface reduced the metal sputtering yield. This result is due to a fact that nitride compounds have a lower sputtering rate and higher secondary electron emission yields than the metal [16]. The chemical compositions of the CrZrSiN coatings are shown in the table. When N_2 partial pressure increased to 0.31 Pa, the nitrogen content of the coating increased to approximately 55 at %, and the Cr and Zr content decreased to 24 and 13 at %, respectively. However, N_2 partial pressure did not significantly affect the Si content in the coatings.

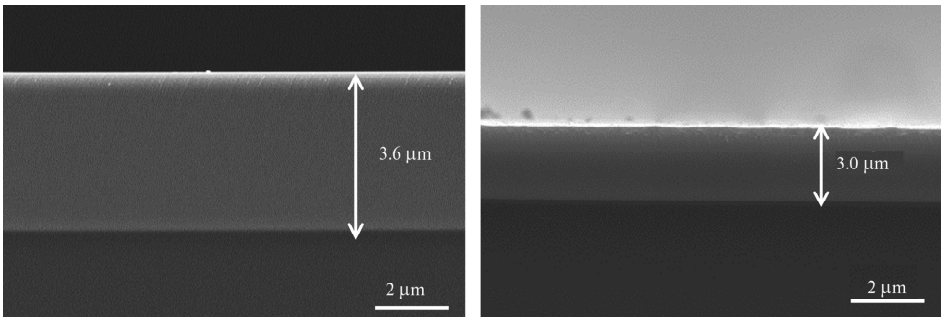

a *b*

Fig. 1. Cross-sectional (FE-SEM) images of CrZrSiN coatings at various N_2 partial pressures of 0.16 (*a*) and 0.31 (*b*) Pa.

Chemical composition of CrZrSiN coatings at various N_2 partial pressures

N_2 partial pressure, Pa	Cr, at %	Zr, at %	Si, at %	N, at %
0.16	33.5	18.8	8.3	39.4
0.21	33.2	18.4	8.1	40.3
0.25	30.1	15.0	9.4	45.5
0.31	23.7	13.0	8.5	54.9

The cross sectional TEM dark-field image of the CrZrSiN coating deposited at N_2 partial pressure of 0.31 Pa is shown in Fig. 2, *a*, and a tiny columnar structure was observed (bright area). To explore the nanocomposite structural details of the CrZrSiN coating, the plan view of the coating was investigated using STEM techniques. Figure 2, *b* presents a Z-contrast STEM image of the CrZrSiN coating deposited at N_2 partial pressure of 0.31 Pa. The STEM image reveals that the crystalline phase (bright area) and the amorphous phase (dark area) coexisted in the nanocomposite structure, and the crystalline grain size and thickness of the amorphous phase were measured to be approximately 4.5±0.3 and 1.0±0.2 nm, respectively. Cr and Si EDS profiles along the inserted line in Fig. 2, *b* are plotted in Figs. 2, *c* and *d*, respectively.

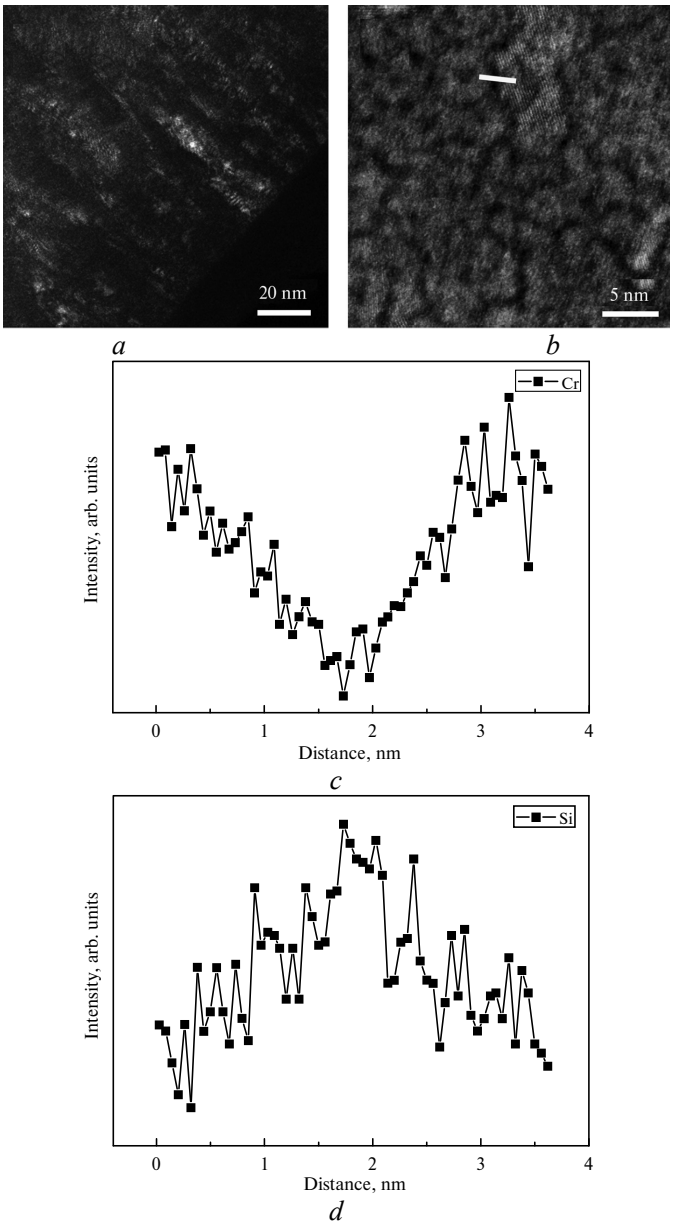

Fig. 2. Cross-sectional dark field TEM image (*a*), plan view STEM image, showing crystalline phase and amorphous phase synthesized at N_2 partial pressure of 0.31 Pa (*b*), Cr lateral concentration profiles (*c*), and Si lateral concentration profiles along the line in Fig. 2, *b* (*d*).

Figure 3 shows the XRD patterns of the as-deposited coatings. The diffraction peaks of the CrZrSiN coatings were observed at the positions shifted toward a lower diffraction angle from the CrN (200) peak. This is because the CrZrN consisted of a solid solution with Zr atoms [17]. Generally, the preferred orientation of the CrZrN coating was at the (111) plane. This is because the crystal structure of the CrZrN coating was of the fcc NaCl type with a minimum strain energy plane of (111). However, the CrZrN (200) peak was observed in this work. The decision of preferred orientation of the coating corresponded to the plane with the lowest energy. Oh et al. [18] reported that the competing planes in the TiN

coating were (200) with the lowest surface energy and (111) with the lowest strain energy. The preferred orientation is determined via a competition between the surface and the strain energy. The overall energy of the (200) plane is lower than that of the (111) under the critical thickness. However, as the strain energy becomes dominant over the critical thickness, the (111) plane possesses lower overall energy [18]. In the nanocomposite structure, the crystalline phase is limited in terms of increasing over the critical size caused by the surrounding amorphous phase. Consequently, in the current study, the preferred orientation was CrZrN (200) in the CrZrSiN coatings, and the peak intensity decreased due to the influence of the amorphous phase with increasing N_2 partial pressure. The SiN_x diffraction peaks were not detected, which suggests that the SiN_x phase in the coating existed in an amorphous state.

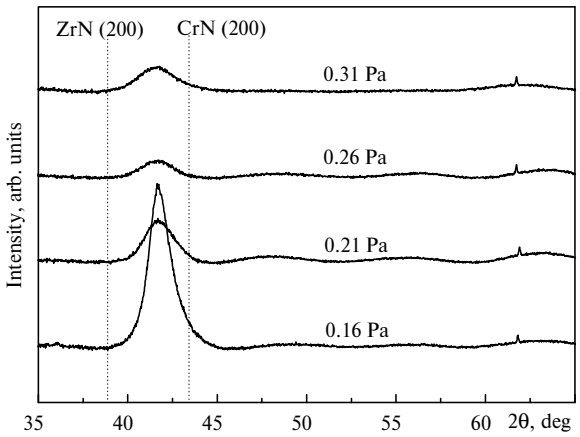

Fig. 3. X-ray diffraction patterns of the as-deposited CrZrSiN coatings with various N_2 partial pressures.

In order to clarify the bonding status of the amorphous phase comprising the CrZrSiN coatings, XPS analyses were performed. Figure 4 showed the XPS spectra near the binding energy of N_{1s} for coatings for N_2 partial pressure of 0.16 Pa. All of the XPS spectra were analyzed using Gaussian fit to acquire the chemical bonding information of the film. The N_{1s} spectra revealed the presence of the two-peak characteristics of nitrogen in the CrZrN crystalline phase and the SiN_x amorphous phase with binding energies at approximately 396.7 and 397.7 eV, respectively. As N_2 partial pressure increased, the ratio of the peak's SiN_x to CrZrN intensity changed from 0.13 to 0.16, which indicated that a volume fraction of the SiN_x phase increased. It was reported previously that as the amorphous phase in the coating increased with the addition of the Si content, the SiN_x peak in the XPS result increased relatively [19]. The result of XRD and XPS proved that N_2 partial pressure influenced the distribution of the crystalline phase and amorphous phase in CrZrSiN coatings.

An indentation test was conducted to investigate the effect of the SiN_x volume fraction change on the mechanical properties of the coatings. The hardness and elastic modulus of the CrZrSiN coatings deposited at the various N_2 partial pressures are shown in Fig. 5. The results show that the hardness of the CrZrSiN coatings gradually decrease from 38 to 30 GPa with increasing N_2 partial pressure. The hardness enhancement in the nanocomposite coatings was due to the combination of the nanocrystalline phase, in which dislocations were hardly able to emerge, and the amorphous phase, which avoids grain boundary sliding. In other

words, the usual mechanisms that cause plastic deformation and crack propagation in conventional polycrystalline are hindered in the nanocomposite coatings due to the interface strain strengthening effect. A very thin amorphous layer between the nanocrystalline phases inhibited the dislocation movement so that it helped to enhance the hardness of the nanocomposite coatings. Musil reported that nanocomposite coating with 1 to 2 amorphous monolayers were to enhanced the hardness of the nanocomposite coating extensively [20]. Also Patscheider et al. conclude that a nanocomposite coating with an amorphous phase of approximately 0.4 nm in thickness, which corresponds to four chemical bond lengths in SiN_x shows the maximum hardness [21]. In this study, the amount of the SiN_x phase increased with increasing N_2 partial pressure, and the amorphous layer thickness became increased from 0.5±0.2 nm at 0.16 Pa to 1.0±0.2 nm at 0.31 Pa. Consequently, according to Musil and Patscheider et al. the strengthening effect from the amorphous phase at the interface reduced, resulting in the decrease of the hardness in this CrZrSiN coatings.

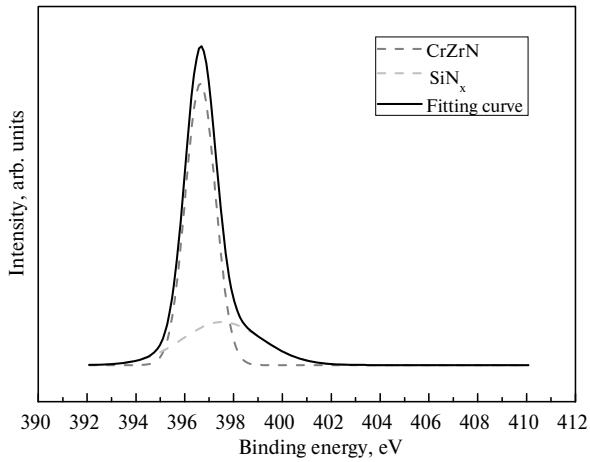

Fig. 4. XPS spectrum (N_{1s} core) of CrZrSiN coatings with N_2 partial pressure of 0.16 Pa.

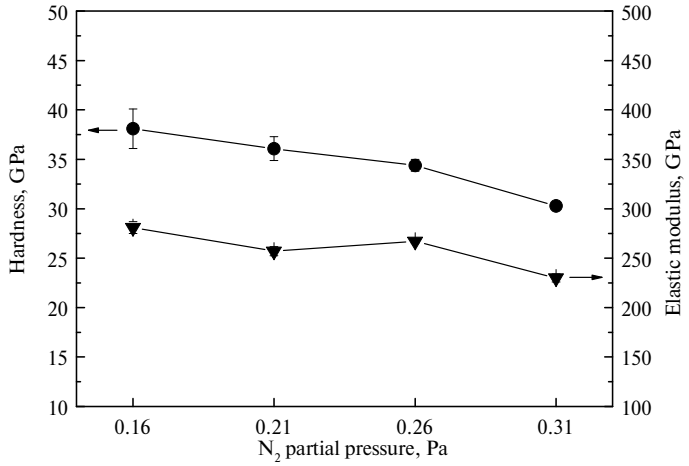

Fig. 5. Hardness and elastic modulus of CrZrSiN coatings with various N_2 partial pressures.

To identify the thermal stability of the CrZrSiN coating, annealing tests were carried out in air for 30 min. The variation of hardness on the CrZrSiN coatings

after the annealing test is presented in Fig. 6, *a*. At all conditions, the hardness values of approximately 30 GPa were maintained up to 800 °C. Kim et al. [22] reported that, the hardness of the CrZrN coatings decreased from 32 to 22 GPa after annealing at 500 °C, so that the CrZrSiN coating showed better thermal stability than the CrZrN coating. This is because the addition of Si to synthesize the amorphous phase was excellent method of maintaining the hardness of the coating at high temperature [13, 23]. From room temperature to 800 °C, the hardness values of the CrZrSiN coatings decreased gradually, but the values decreased rapidly to 18 GPa after annealing at 900 °C. This decrease of the hardness could be attributed to the effect of the annealing treatment on the residual stress in the coating. The drastic change of hardness over 800 °C could be attributed to the formation of the Cr_2O_3 phase on the CrZrSiN coating as shown in the Raman spectra of as-deposited and heat-treated CrZrSiN coating in Fig. 6, *b*. There was no significant change in the nature of the Raman spectrum up to 800 °C. However, weak peaks of the Cr_2O_3 centered at 549 and 613 cm^{-1} [23] appeared at a temperature of 900 °C. Additional peaks observed at 306 and 348 cm^{-1} correspond to Cr_2O_3 [23]. Therefore, the rapid decreasing of hardness was a result of the formation of a Cr_2O_3 phase, which had lower hardness of 14 GPa [24] compared to the CrZrSiN

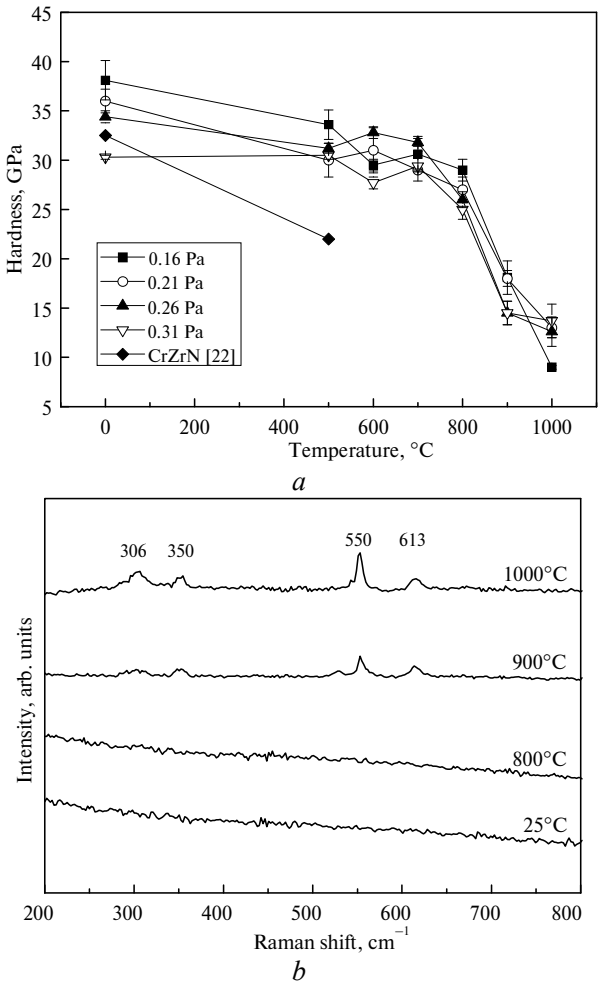

Fig. 6. Hardness (*a*), and Raman spectrum variation (*b*) of CrZrSiN coatings after annealing test for 30 min.

coating. Also, the thermal stability of the CrZrSiN coating was not affected significantly by its nitrogen content. Kim et al. reported that the thermal stability of the CrZrSiN coating enhanced with increasing Si content, and the hardness of the CrZrSiN coating with Si content of more than 13.5 at % was maintained up to 1000 °C [13]. In this study, the Si contents of all CrZrSiN coatings were in the range of 8.1 to 9.4 at % and these amounts of Si is not enough to ensure the enhanced thermal stability of the Si-containing CrZrSiN coatings.

CONCLUSIONS

CrZrSiN nanocomposite coatings at various N_2 partial pressures were synthesized successfully using unbalanced magnetron sputtering and studied with regard to their microstructure and mechanical properties. The CrZrSiN coatings showed a typical nanocomposite structure, in which CrZrN nanocrystalline grains were embedded in a SiN_x amorphous phase. XRD results showed that the CrZrSiN coatings exhibited (200) reflections of the cubic CrZrN phase and the peak intensity decreased at high N_2 partial pressures. In XPS studies, the N_{1s} core spectra revealed that the CrZrSiN coating consisted of a CrZrN nanocrystalline phase and SiN_x phase, and that the amorphous phase increased with increasing N_2 partial pressure. The CrZrSiN coatings exhibited a maximum hardness and elastic modulus of 38 GPa and 280 GPa at a N_2 partial pressure 0.16 Pa, respectively. The hardness and elastic modulus of the coatings decreased with the increase of the N_2 partial pressure. After the annealing test, the CrZrSiN coatings maintain their hardness at the 800 °C, but the hardness decreased rapidly over 900 °C due to the formation of a Cr_2O_3 phase. The Raman spectrum showed that the onset of the oxidation of the CrZrSiN coating with Si content in the range of 8.1 to 9.4 at % was 900 °C, which is considered to be the thermal stability limit of the coatings.

This research was supported by a grant from the Advanced Technology Center (ATC) Program funded by the Ministry of Trade, Industry& Energy of Korea.

Досліджено вплив парціального тиску N_2 в процесі незбалансованого магнетронного розпилення на мікроструктуру, твердість і термостабільність нанокомпозитного покриття CrZrSiN. Отримано типову структуру нанокомпозиту, що складається з кристалічної і аморфної фази, розподіл цих фаз змінюється зі збільшенням парціального тиску N_2. В N_{1s}-спектрах присутні два піки, що характеризують азот в фазах CrZrN і SiN_x, відношення інтенсивностей SiN_x- і CrZrN-піків зростає зі збільшенням парціального тиску N_2, що свідчить про збільшення аморфної фази в нанокомпозитних мікроструктурах. У міру збільшення парціального тиску N_2, твердість покриття CrZrSiN знизилася з 38 до 30 ГПа в зв'язку зі збільшенням кількості аморфної фази SiN_x. Після випробування на термічну стабільність значення твердості цх CrZrSiN-покриттів підтримували на рівні ~30 ГПа до температури 800 °С, але твердість швидко знижувалась до 18 ГПа після відпалу при температурі 900 °С. Різка зміна твердості при температурі понад 900 °С пов'язана з утворенням фази Cr_2O_3 в покритті CrZrSiN.

***Ключові слова**: покриття, нанокомпозит, мікроструктура, аморфна фаза.*

Исследовано влияние парциального давления N_2 в процессе несбалансированного магнетронного распыления на микроструктуру, твердость и термостабильность нанокомпозитного покрытия CrZrSiN. Получена типичная структура нанокомпозита, состоящая из кристаллической и аморфной фази, распределение этих фаз изменилось с увеличением парциального давления N_2. В N_{1s}-спектрах присутствовали два пика, характеризующие азот в фазах CrZrN и SiN_x, отношение интенсивностей SiN_x- и CrZrN-пиков возрастает с увеличением парциального давления N_2, что свидетельствует об увеличении аморфной фазы в нанокомпозитных микроструктурах. По мере увеличения парциального давления N_2, твердость покрытия CrZrSiN снизилась с 38 до 30 ГПа в связи

с увеличением количества аморфной фазы SiN_x. После испытания на термическую стабильность значения твердости CrZrSiN-покрытий поддерживали на уровне ~30 ГПа до температуры 800 °С, но твердость быстро снижалась до 18 ГПа после отжига при температуре 900 °С. Резкое изменение твердости при температуре свыше 900 °С связано с образованием фазы Cr_2O_3 в покрытии CrZrSiN.

***Ключевые слова**: покрытие, нанокомпозит, микроструктура, аморфная фаза.*

1. *Zou C. W., Zhang J., Xie W. et al.* Synthesis and mechanical properties of quaternary Ti–Cr–Si–N nanocomposite coatings deposited by closed field unbalanced middle frequency magnetron sputtering // J. Alloy. Comp. – 2012. – **529**. – P. 52–57.
2. *Lin J., Wang B., Ou Y., Sproul W. D. et al.* Structure and properties of CrSiN nanocomposite coatings deposited by hybrid modulated pulsed power and pulsed dc magnetron sputtering // Surf. Coat. Technol. – 2013. – **216**. – P. 251–258.
3. *Diserens M., Patcheider J., Levy F.* Mechanical properties and oxidation resistance of nanocomposite TiN–SiN_x physical-vapor-deposited thin films // Ibid. – 1999. – **120**–**121**. – P. 158–165.
4. *Mae T., Nose M., Zhou M., Nagae T.* The effects of Si addition on the structure and mechanical properties of ZrN thin films deposited by an r.f. reactive sputtering method // Ibid. – 2001. – **142**–**144**. – P. 954–958.
5. *Barshilia H. C., Deepthi B., Srinivas G., Rajam K. S.* Sputter deposited low-friction and tough Cr–Si_3N_4 nanocomposite coatings on plasma nitrided M2 steel // Vacuum. – 2012. – **86**. – P. 1118–1125.
6. *Barshilia H. C., Deepthi B. Rajam K. S.* Deposition and characterization of CrN/Si_3N_4 and CrAlN/Si_3N_4 nanocomposite coatings prepared using reactive DC unbalanced magnetron sputtering // Surf. Coat. Technol. – 2007. – **201**. – P. 9468–9475.
7. *Philippon D., Godinho V., Nagy P. M. et al.* Endurance of TiAlSiN coatings: Effect of Si and bias on wear and adhesion // Wear. – 2011. – **270**. – P. 541–549.
8. *Castaldi L., Kurapov D., Reiter A. et al.* High-temperature phase changes and oxidation behavior of Cr–Si–N coatings // Surf. Coat. Technol. – 2007. – **202**. – P. 781–785.
9. *Veprek S., Veprek-Heijiman M. G. J., Karvankova P., Prochazka J.* Different approaches to superhard coatings and nanocomposites // Thin Solid Films. – 2005. – **476**. – P. 1–29.
10. *Zhang Y., Yang Y., Zhai Y., Zhang P.* Effect of negative substrate bias on the microstructure and mechanical properties of Ti–Si–N films deposited by a hybrid filtered cathodic arc and ion beam sputtering technique // Appl. Surf. Sci. – 2012. – **258**. – P. 6897–6901.
11. *Chen T., Xie Z., Gong F. et al.* Correlation between microstructure evolution and high temperature properties of TiAlSiN hard coatings with different Si and Al content // Appl. Surf. Sci. – 2014. – **314**. – P. 735–745.
12. *Tritremmel C., Daniel R., Lechthaler M. et al.* Influence of Al and Si content on structure and mechanical properties of arc evaporated Al–Cr–Si–N thin films // Thin Solid Films. – 2013. – **534**. – P. 403–409.
13. *Kim Y. S., Kim G. S., Lee S. Y.* Thermal stability and electrochemical properties of CrZr–Si–N films synthesized by closed field unbalanced magnetron sputtering // Surf. Coat. Technol. – 2009. – **204**. – P. 978–982.
14. *Lee S. Y., Kim Y. S., Kim G. S.* Thermal stability and tribological properties of CrZr–Si–N films synthesized by closed field unbalanced magnetron sputtering // J. Vac. Sci. Technol. A. – 2009. – **27**. – P. 867–872.
15. *Lee J. W., Chang S. Y., Chen H. W. et al.* Microstructure, mechanical and electrochemical properties evaluation of pulsed DC reactive magnetron sputtered nanostructured Cr–Zr–N and Cr–Zr–Si–N thin films // Surf. Coat. Technol. – 2010. – **205**. – P. 1331–1338.
16. *Han Z., Tian J., Lai Q. et al.* Effect of N_2 partial pressure on the microstructure and mechanical properties of magnetron sputtered CrN_x films // Ibid. – 2003. – **162**. – P. 189–193.
17. *Kim G. S., Kim B. S., Lee S. Y., Hahn J. H.* Structure and mechanical properties of Cr–Zr–N films synthesized by closed field unbalanced magnetron sputtering with vertical magnetron sources // Ibid. – 2005. – **200**. – P. 1669–1675.
18. *Oh U. C., Je J. H.* Effects of strain energy on the preferred orientation of TiN thin films // J. Appl. Phys. – 1993. – **74**. – P. 1692–1696.
19. *Lee H. Y., Jung W. S., Han J. G. et al.* The synthesis of CrSiN film deposited using magnetron sputtering system // Surf. Coat. Technol. – 2005. – **200**. – P. 1026–1030.

20. Musil J. Hard nanocomposite coatings: Thermal stability, oxidation resistance and toughness // Ibid. – 2012. – **207**. – P. 50–65.
21. *Patscheider J., Zehnder T., Diserens M.* Structure-performance relations in nanocomposite coatings // Ibid. – 2001. – **146**–**147**. – P. 201–208.
22. *Kim S. M., Kim B. S., Kim G. S. et al.* Evaluation of the high- temperature characteristics of the CrZrN coatings // Ibid. – 2008. – **202**. – P. 5521–5525.
23. *Barshilia H. C., Rajam K. S.* Raman spectroscopy studies on the thermal stability of TiN, CrN, TiAlN coatings and nanolayered TiN/CrN, TiAlN/CrN multilayer coatings // J. Mater. Res. – 2004. – **19**. – P. 3196–3205.
24. *Pang X., Gao K., Luo F. et al.* Annealing effects on microstructure and mechanical properties of chromium oxide coatings // Thin Solid Films. – 2008. – **516**. – P. 4685–4689.

Received 05.08.15